Type of contribution:
Editorial
▶ Research Paper
Case Study
Review Paper
Scientific Data
Report of Tech. Application

mesi
e-issn. 2798-5245

Mechanical Engineering
for Society and Industry
Vol. 5, No. 1 (2025) pp 169-181
https://doi.org/10.31603/mesi.12733

The analysis of semiconducting charateristic of rice husk-based carbon nanomaterial bio-activated by pineapple peel juice

Ni Made Dwidiani[1], Ngakan Putu Gede Suardana[1], I Nyoman Gede Wardana[2]*, Willy Satrio Nugroho[2], I Gusti Ketut Puja[3], Wayan Nata Septiadi[1], I Gusti Ngurah Nitya Santhiarsa[1], Si Putu Gede Gunawan Tista[1]

[1] Department of Mechanical Engineering, Universitas Udayana, Badung 80361, **Indonesia**
[2] Department of Mechanical Engineering, Universitas Brawijaya, Malang 65145, **Indonesia**
[3] Department of Mechanical Engineering, Universitas Sanata Dharma, Sleman 55281, **Indonesia**
✉ wardana@ub.ac.id

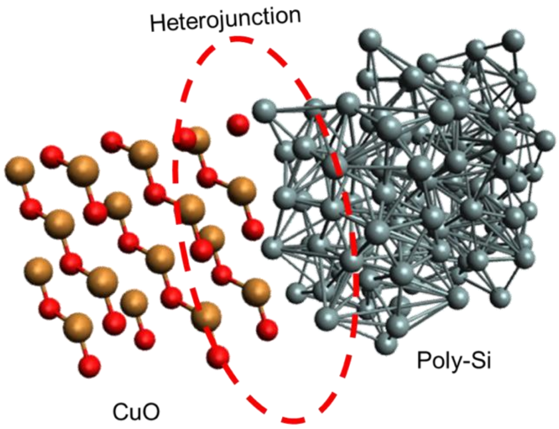

Highlights:

- SCNM and FCNM show tailored nanostructures with surface cracks induced by bromelain activation.
- High CuO and Si content in SCNM enhances its semiconductor and photoactive properties.
- Strong UV absorption indicates effective photon-triggered electron transport.
- Generates significant photoelectric current, suitable for energy devices and sensors.

Abstract

This study investigates the synthesis and characterization of semiconducting materials derived from rice husk bio-activated by pineapple peel juice, presenting an eco-friendly and sustainable approach. The organic photo-active semiconducting material from rice husk ash (RHA) is synthesized. RHA was activated by immersion in the pineapple juice solution. Distinct structural disparities among RHA, Sunken Carbon nanomaterial (SCNM), and Floating Carbon Nanomaterial (FCNM) materials are revealed through SEM imaging, showcasing the tailored nature of each material. The SEM images also indicate the role of bromelain from the pineapple juice to provide defects on the RHA carbon surface. The crack on the nano particles on the surface of SCNM and FCNM were formed due to the bromelain electrostatic interaction with the surface. Elemental analysis indicates a higher probability of CuO and Si presence in SCNM, suggesting its potential for semiconductor extraction. The Cu to Si ratio implies photoactivity, confirmed by UV-Vis characterization showing absorption peaks in the UV region. FTIR analysis highlights enhanced polar interactions in SCNM and FCNM, attributed to the activation process involving bromelain in pineapple juice. The photoelectric effect testing shows FCNM and SCNM generates more electrical current as exposed to light which. The current was generated due to the electron transport phenomenon of CuO and Si content triggered by photons. The study provides insights into the materials' molecular structures and potential applications in sensors, energy devices, and semiconductor-related technologies, leveraging the unique properties of bio-derived nanomaterials for practical implementation.

Keywords: Semiconducting materials; Rice husk ash; Nanomaterial; Pineapple juice; Photo-active materials

Article info
Submitted:
2024-11-29
Revised:
2025-06-07
Accepted:
2025-06-22

Publisher
Universitas Muhammadiyah Magelang

1. Introduction

The exploration of novel materials with semiconducting properties is crucial for advancing various technological application [1]. This study investigates the semiconducting characteristics of rice husk-based carbon nanomaterials bio-activated by pineapple peel juice were originated. The utilization of agricultural by-products, such as rice husk, coupled with the bio-activation process using pineapple peel juice, not only presents an eco-friendly approach but also introduces a sustainable and cost-effective pathway to synthesize semiconducting nanomaterials [2]. The unique combination of rice husk-derived carbon and the bio-activation by pineapple peel juice offers an intriguing synergy that may result in tailored electronic properties suitable for applications in sensors, energy devices, or other semiconductor-related technologies. This study observes the semiconducting attributes of this bio-derived nanomaterial, shedding light on its potential for practical implementation in a range of cutting-edge technologies.

Semiconducting materials has a key role in energy transition and sustainability. Energy conversion device always bound to efficiency. In fluid based energy conversion device such as turbine, the efficiency determined by its design. For example, the nozzle angle of second stage cross-flow turbine design determines its efficiency [3]. On the chemical energy conversion, the heat transfer determines the quality of the conversion. The example is the variation of calorific value in pyrolysis process due to the additional materials with different thermal capacity [4]. Semiconductor materials always required to build the control device for energy conversion [5]. Therefore, the finding of a novel semiconducting material remains an actual issue.

The wide application of nanomaterials has emerged as a transformative force across diverse scientific and technological domains. Nanostructured materials, characterized by their unique properties at the nanoscale, are increasingly finding applications in fields ranging from medicine and electronics to energy and environmental science. In medicine, nanoparticles are revolutionizing drug delivery systems, allowing for targeted and controlled release of therapeutic agents [6]. The article [6] demonstrates the use of biodegradable periodic mesoporous organosilicas (BPMOs) and metal-organic frameworks (MOFs) as a vehicle to deliver the therapeutic agent to the targeted cells. In electronics, the utilization of nanomaterials has led to the development of more efficient and miniaturized devices, paving the way for advancements in computing and telecommunications. Article [7] reviews the application of 2D nanomaterials which found the high anisotropy, effective surface area, mechanical strength, plasmonic, electron confinement, and optical properties of such materials. The study [8] reports the energy sector benefits from nanomaterials in the form of enhanced catalysis, improved solar cells, and energy storage devices. Moreover, in environmental science, nanomaterials are employed for pollutant removal, sensing, and remediation, contributing to sustainable solutions. This comprehensive integration of nanomaterials underscores their versatility and underscores their pivotal role in shaping the forefront of scientific and technological progress.

The photoactive organic materials have been widely used in digital electronics. Previously, the development of hydrogen photocatalyst utilizing the compact disc (CD) waste has successfully provide cheap hydrogen generator as stated in article [9]. Meanwhile, the article [10] provides the CD-R based electrocatalyst which can be controlled using the stored information bits sequences. The CD-R information was chiseled by optical photoelectric effect that changes the cyanine dye constellation on its surface as stated by article [11]. The article [12] reports the organic content of CD-R which is Bisphenol-A contain aromatic benzene which help to disrupt the water molecules stability due to aromatic magnet effect. Another benefit of the organic CD-R based electrocatalyst is it forms hydrophobic surface on the anode which protect the carbon anode from carbon corrosion enable anode to sustain longer oxygen evolution reaction (OER) as reported in article [13]. The article [14] as the continuation of the CD-R based organic semiconducting electrocatalyst cyanine dye (II) development shows the magnetic response which improves the charge transfer during magnetic field exposure. The magnetic response of CD-R based organic electrocatalyst is better compared to chaotic flux magnetic induction reported in study [15]. Therefore, organic semiconducting material has been play a significant role in hydrogen production research development.

Organic optoelectronic materials possess much novel functionality. The article [16] shows organic photovoltaics, is poly(3,4-ethylenedioxythiophene) (PEDOT) responsible for selective hole trapping on ZnO surface which enable oxidation control on thin film electrode. The article [17] reports Poly(methyl methacrylate) (PMMA) embedded on styrene copolymer resists ultraviolet-C (UV-C) which shows the improve in electrical resistance. Furthermore, study [18] reviews the application of transparent conducting electronics (TCE) including organic and perovskite solar cells, organic light emitting diodes, supercapacitors, electrochromic devices. The study found the main benefits of organic optoelectronics is its electron-hole interaction flexibility.

Semiconducting organic nanoparticles have emerged as a highly promising class of materials, garnering significant attention in the realm of nanotechnology and electronic device development. Their unique properties, derived from organic compounds, offer advantages such as tunable electronic characteristics, flexibility, and solution-processability [19]. Article [20] reports these nanoparticles, typically composed of conjugated polymers or small organic molecules, exhibit semiconducting behavior, making them well-suited for applications in organic electronics, photovoltaics, and sensors. The study [21] states the inherent versatility in their chemical structures allows for precise control over their electronic properties, enabling the design of customized materials with tailored energy levels and charge transport capabilities. The synthesis, characterization, and applications of semiconducting organic nanoparticles, this burgeoning field holds immense promise for the realization of next-generation electronic devices with improved performance and functionality. Previously, the photoelectric activity of the rice husk carbon nanomaterials with pineapple juice have been predicted [22]. This article confirms the organic semiconducting properties of a material made of rice husk with pineapple juice bio activator.

This study explores the potential application of the synthesized organic semiconducting material. The aim of this study is to synthesize and observe photoactive material based on rice husk-based nanomaterial activated by-pineapple peel juice. The photo-activity of the material analyzed through photoelectric experiment and light-based characterization. The photo-activity of the material assessed based on the generated photo current and the characterization results. This study outlines the potential of the synthesized material as the photo semiconducting material.

2. Materials and Method

The first step to provide alternative synthesis method of photoactive organic semiconductor based on RHA is to acquire the rice husk. We obtained the rice husk from Tabanan, Bali, Indonesia which has been readily available as agricultural waste. The rice husks were thoroughly cleaned and subjected to grinding until reaching a particle size of 200 mesh. The grinding process aims to enhance the surface area and reactivity of the rice husk, providing an optimal starting point for subsequent activation and transformation into semiconducting carbon nanomaterials [23].

Following the grinding process, the rice husk particles were subjected to High-Energy Milling (HEM) for 1 million cycles. The HEM equipment was a custom-made shaker mill with 5 mm diameter hardened steel ball. HEM was employed to induce mechanical activation, facilitating the breakdown of crystalline structures and promoting the development of a highly reactive carbon matrix. The controlled mechanical forces imparted during HEM contribute to the homogenization and refinement of the material's structure, setting the stage for enhanced reactivity [24]. Hence, HEM plays a pivotal role in creating a suitable precursor for the subsequent bioactivation process.

The main objective to perform alternative synthesis method is by using natural organic solvent which is the pineapple peel juice. The pineapple peel juice as the bio-activator in the synthesis of semiconducting carbon nanomaterials from rice husk-derived activated carbon, was prepared through a meticulous process. Fresh, ripe pineapples obtained from local market Jimbaran were selected and peeled. The pineapple peel was chopped into chunk and added to blender and then pressed to preserve enzymatic activity. The targeted content was bromelain, a mixture of proteolytic enzymes, is known for its ability to hydrolyze peptide bonds in proteins [25]. We immerse 45 gram of rice husk activated ash in 259 ml of pineapple peel juice.

The rice husk ash undergoes a unique bio-activation process by immersion in pineapple peel juice at a controlled temperature of 60 °C for 4 hours. Pineapple peel juice, rich in enzymatic and acidic components, serves as a bio-activator, introducing functional groups and heteroatoms to the carbon matrix. This bio-activation step is crucial for tailoring the surface chemistry of the material, potentially imparting semiconducting properties. The controlled conditions ensure the efficient interaction between the organic components of the pineapple juice and the activated carbon, paving the way for the formation of semiconducting structures.

Subsequent to the bioactivation process, the material is thoroughly rinsed to remove residual pineapple juice and reaction by-products. The rinsing step ensures the removal of any extraneous components that may interfere with the semiconducting properties of the final product. The products were rinsed using deionized water. The next step is separating small and big size carbon nanomaterial (CNM) by depositing the material into water in a tube and the stirred well for 8 hours. The small or floating material (FCNM) we re obtained by pouring the water contained FCNM and were then dried out as well as the residual that sunk in the bottom of the tube (SCNM). Both FCNM and SCNM were analyzed and characterized. The semiconducting carbon nanomaterial obtained was thoroughly examined using scanning electron microscopy (SEM) to assess its structural and morphological properties. This technique provides detailed insights into the effectiveness of the bioactivation process in inducing semiconducting characteristics. The SEM was performed for RHA, SCNM, and FCNM samples with 30000X magnification. The SEM imaging device was JSM-6510 LA and used in high vacuum mode.

To account for the surface-sensitive nature of EDS, complementary characterization techniques were employed to validate the presence and role of semiconducting elements in the bulk phase. EDS analysis was conducted in conjunction with UV-Vis spectroscopy, FTIR, and photocurrent measurements to corroborate the surface elemental data with optical and functional properties. While EDS primarily detects surface-level composition, UV-Vis absorption spectra and photoresponse behavior provide insight into the electronic transitions and bandgap features characteristic of bulk semiconducting materials. Furthermore, FTIR analysis was used to identify chemical bonding patterns and functional groups indicative of oxide formation. This multi-technique approach enhances the reliability of the EDS results and ensures a more comprehensive understanding of the material's bulk semiconducting properties.

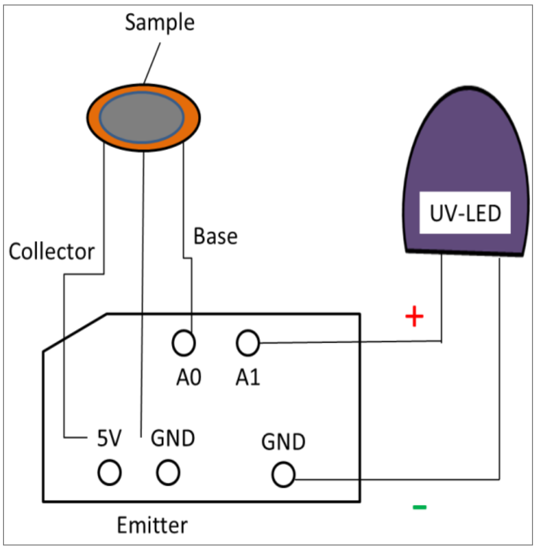

Figure 1. The photo current measurement setup

The photosensitivity analysis was performed by direct experiment and UV-Vis spectroscopy characterization. The photo current measurement device was made using an Arduino UNO R3 microcontroller (Arduino, Italy) and a phototransistor. The experimental setup of the photo current measurement is shown in **Figure 1**. The phototransistor collector was connected to the Arduino's 5V output, emitter to ground, and base to an analog input pin (A0). The tested material was placed on top of the phototransistor using a wet cotton bud. The phototransistor then radiated with 365 nm UV-Light from a UV Light emitting diode (LED). Each sample was radiated in 300 seconds. The output voltage was subsequently recorded in data logger.

The photo current measurement device was made using an Arduino UNO R3 microcontroller (Arduino, Italy) and a phototransistor. The experimental setup of the photo current measurement is shown in **Figure 1**. The phototransistor collector was connected to the Arduino's 5V output, emitter to ground, and base to an analog input pin (A0). The tested material was placed on top of the phototransistor using a wet cotton bud. The phototransistor then radiated with 365 nm UV-Light from a UV Light emitting diode (LED). Each sample was radiated in 300 seconds. The output voltage was subsequently recorded in data logger.

UV-Vis spectroscopy Shimadzu UV-2600 and Fourier-Transform Infrared (FTIR) spectroscopy Shimadzu/IR Prestige 21 were employed as integral components of the materials and methods in this study. UV-Vis spectroscopy was utilized to examine the optical properties of the synthesized semiconducting carbon nanomaterial. The absorption spectra obtained through UV-Vis spectroscopy provided valuable information regarding the electronic transitions and bandgap characteristics, offering insights into the material's semiconducting behavior. Additionally, FTIR spectroscopy was employed to analyze the chemical composition and functional groups present in the nanomaterial. The infrared spectra obtained through FTIR facilitated the identification of specific bonds and molecular vibrations induced by the bioactivation process. Together, UV-Vis and FTIR spectroscopy played a crucial role in characterizing the structural, electronic, and chemical aspects of the semiconducting carbon nanomaterial, contributing to a comprehensive understanding of its properties and paving the way for potential applications in advanced technologies.

3. Results and Discussion

3.1. Morphology and elemental characterizations

The SEM imaging results (**Figure 2**) shows distinct structural disparities among RHA, SCNM, and FCNM materials. The SEM images depict unique morphologies, showcasing variations in surface topography and particle arrangements. These structural differences are indicative of the diverse synthesis processes and treatment methods employed, underscoring the tailored nature of each material. In **Figure 2a** the RHA sample consists of a single large microstructure with some smaller microstructures attached on it. Meanwhile, in **Figure 2b** the SCNM consists of a dense structure with irregular surfaces. The irregularities were in the form of wrinkles and bumps. The FCNM microstructures are smoother compared to SCNM (**Figure 2c**).

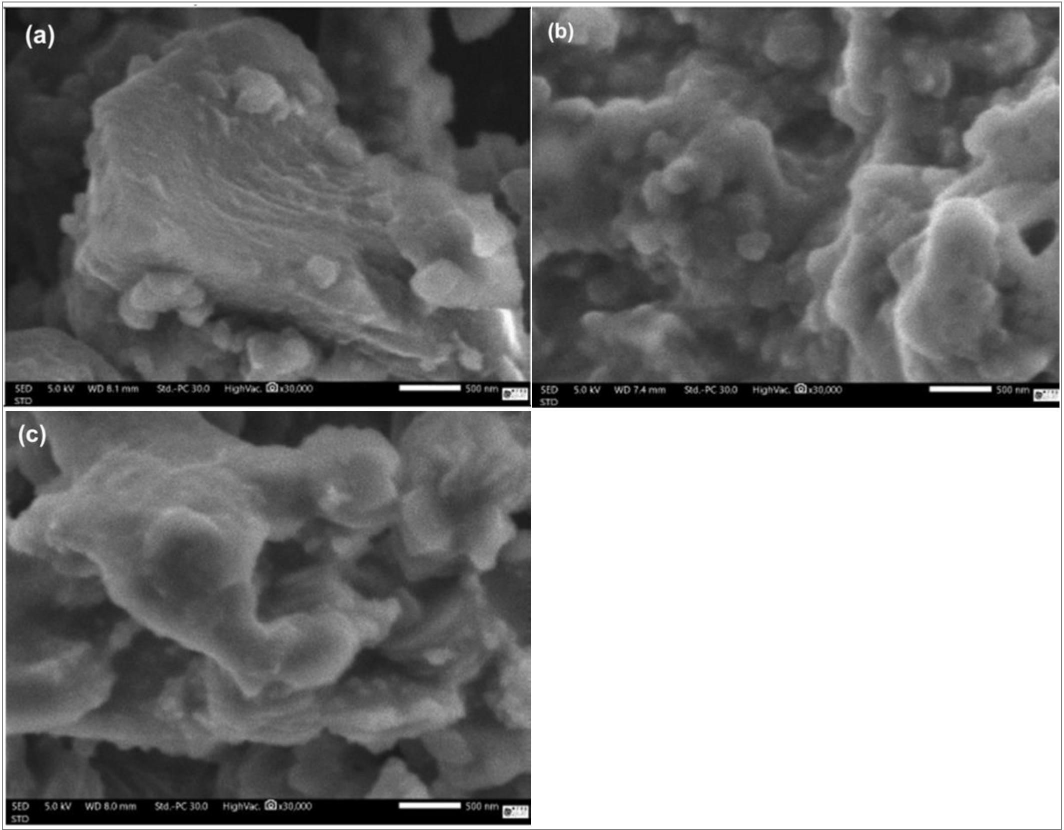

Figure 2. The morphology SEM images of: (a) RHA; (b) SCNM; (c) FCNM

The EDS characterization results show the atomic composition on each sample surface (**Figure 3**). The RHA sample mainly consists of carbon (C) with fewer silicon (Si) and some other elements in 10:3 carbon-silicon ration (**Figure 3a**). The SCNM sample contain more Si instead of carbon with 5:9 ratio. Also, the SCNM contain Ferrous atom (Fe) and little bit of Al atom as seen in **Figure 3b**. The FCNM contains carbon to silicon ratio of 9:4 and also with copper (Cu) atom.

The SCNM and FCNM shows enhanced photo-active performance. The structural change triggers the molecular change which modify the electron configuration [26]. The irregularity of the microstructure surfaces indicates the density of the sample. More wrinkles on the sample means the sample is denser as shown by the SCNM and FCNM (see **Figure 2**). The SCNM is heavier than FCNM which enable it to penetrate through the liquid film causes it to sink in the solution. The mass of a material defined by its density which reflect the amount of mass in a given volume [27]. Density of an object defined by the type of the material which has different specific mass and specific volume [28]. The lighter FCNM was held on the surface as it is affected by the buoyancy [29]. Lighter than air objects produce movements when response Buoyancy [30]. Therefore, the FCNM and SCNM may have different element or functional groups composition due to its Buoyancy response. However, contact surface area defines the Buoyancy response. For example, ship with a high density material still can float due to the right design [31]. The wrinkles of SCNM with denser structure have a smaller contact surface area. The smaller contact surface area distributes greater pressure which exerts stronger force against cohesion on water surface [32]. Therefore, the greater surface and higher density elements of SCNM make it sink.

Bromelain's proteolytic activity plays a pivotal role in breaking down proteinaceous components within the activated carbon, exposing reactive sites, and increasing surface area [33]. Additionally, the acidic environment created by bromelain contributes to the formation of oxygen-containing functional groups on the carbon surface, potentially influencing semiconducting behavior. Bromelain's molecular structure is consists of few aromatic rings with couple of OH functional groups attached to it [34]. Hence, the interaction of the RHA with water is enhanced by

Bromelain's. Bromelain captures the polar impurities on RHA through electrostatic interaction. Therefore, the activation mechanism of RHA was through the cohesion between water content of the pineapple juice with the captured impurities. As a result, the interaction generates crack such as seen in **Figure 2**.

The presence of pineapple-peel juice affects the microsturcure of the SCNM and FCNM. Bromelain as the main enzyme of pineapple-peel juice modifies the protein that present in RHA. As a result, the microstructures were modified by the introduction of defects on its surface (see **Figure 2**). The electrostatic interaction between bromelain and the protein trace on carbon microstructure induces crack on microstructure surface. As a result, the carbon becomes activated due to the separated surface structure.

Besides, Pineapple peel juice as an organic solvent has a less harmful effect to the environment. Mainly, the inorganic strong acids were used to extract organic compound in biomass or organic substrate based energy production. For example, as reported in the article [35], the HCl-bentonite immersion was effective as a pretreatment to decompose biomass based substrate such as corn cob to produce biochar from pyrolysis. Organic acid traces in feedwater are well known to reduce soil quality due to nutrient deficiency [36]. The phytoremediation process is required to removes the contaminant from the soil and the water.

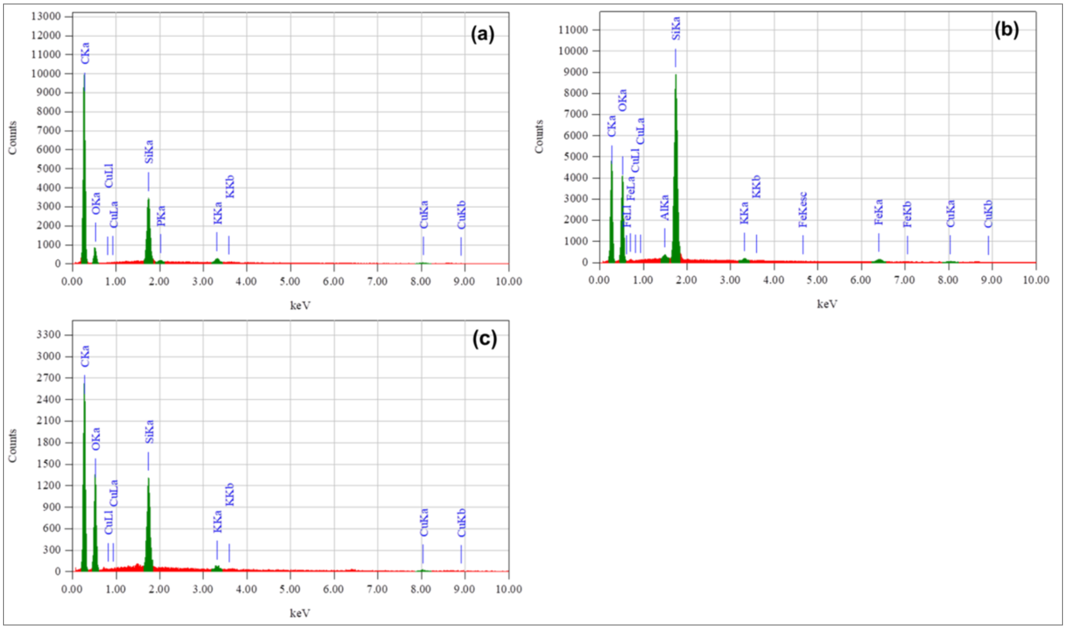

Figure 3. The atomic composition revealed by EDS of: (a) RHA; (b) SCNM; (c) FCNM

3.2. The Detection of Photosensitive elements

The elemental ratio determines the functional properties of the material. Therefore, we observe the Cu and Si ratio of each sample as seen in a bar chart in **Figure 4**. The presence of Cu and Si indicates the semiconducting properties of a material [37]. All samples contain Copper-oxide (CuO) and Si or it is possible to extract both semiconducting materials from the samples. The highest probability of extraction is from SCNM, followed by RHA, and FCNM respectively. Furthermore, the Cu to Si ratio determines the photo activity of a certain material [38].

The UV-Vis characterization confirms the photo-activity of each sample (see **Figure 5**). Every sample light absorption region (RHA, SCNM, and FCNM) were peaked at UV region around 200 nm. This can be seen from the approximately similar location of the curve formation in **Figure 5a** respectively for RHA, SCNM, and FCNM. Therefore, the presence of CuO on each sample can be confirmed. The intensity of the light absorbtion defines the concentration of CuO which shows SCNM and FCNM have similar concentration of CuO semiconducting material.

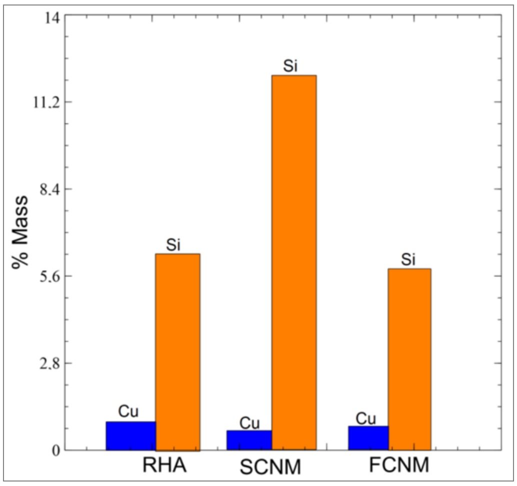

Figure 4. The photo current measurement setup

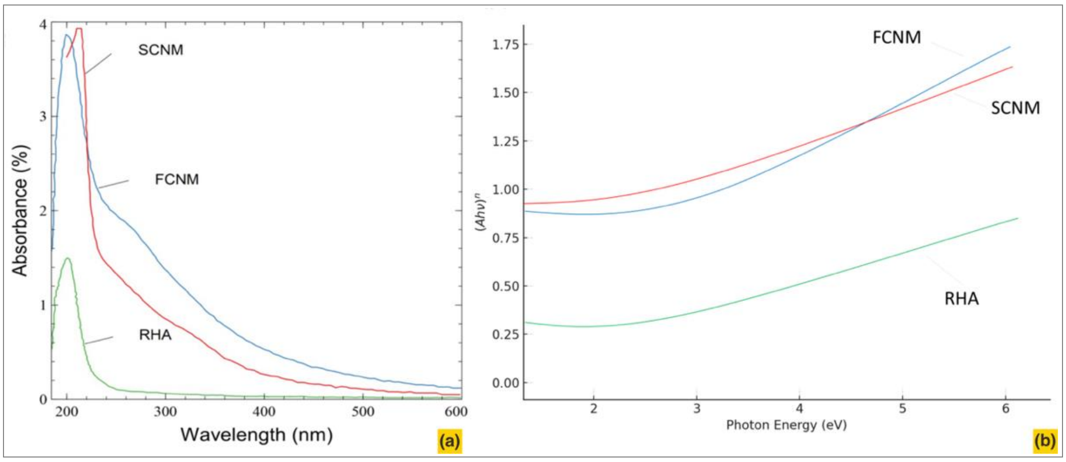

Figure 5. The UV-Vis characterization response of RHA; SCNM; and FCNM: (a) Absorbance plot; (b) Tauc plot

Based on the Tauc plot analysis in **Figure 5b**, the optical band gaps of SCNM, FCNM, and RHA were estimated to assess their photoactivity. The plot of (αhv)2(αhv)^2(αhv)2 versus photon energy (hv) reveals distinct bandgap values for each material, with SCNM exhibiting the lowest bandgap of approximately 3.8–3.9 eV, followed by FCNM with a slightly higher value around 4.0–4.1 eV. This indicates that SCNM has a stronger ability to absorb lower-energy photons. This indicates its favorable for photocatalytic and optoelectronic applications under UV exposure. In contrast, RHA displays a significantly weaker absorption response with a poorly defined linear region, suggesting a larger or disordered bandgap structure exceeding 5 eV, which limits its suitability for photo-induced processes. These findings confirm that the activation and bio-assisted processing enhance the semiconducting behavior of SCNM and FCNM, likely due to the formation of CuO and SiO_2 heterostructures, as supported by the UV-Vis and photocurrent measurements.

The FTIR characterization helps to identify the functional groups of each sanple. The FTIR spectrum of RHA, SCNM, and FCNM are served in **Figure 6a** to **Figure 6c** respectively. Since the frequency spectrum of FTIR is beyond nIR (12500–4000 cm^{-1}), the confirmation of Si –based semiconducting material cannot be determined [39]. However, we found SCNM and FCNM have more OH and CO functional groups. This shows the RHA activation process has changed the overall molecular structure of the SCNM and FCNM. More OH and CO functional groups indicates improved polar interactions such as Keesom, Debye, London dispersion force, and Van der Waals interaction [40].

Silicon-based materials such as silicon wafers or silicon-based compounds exhibit photoactive behavior when exposed to light. CuO also exhibits the similar behavior however with different bandgap region. Si-based material become photoactive in near infrared (nIR) region (800-2500 nm wavelength) and CuO-based material active in ultraviolet (UV) region (200-400 nm wavelength) [41]. The UV-Vis characterization and UV photoelectric testing have confirmed the presence of both elements along with the EDX elemental characterization results in **Figure 3**. Mainly, the UV-Vis result peaked near to 400nm as shown in **Figure 5** which confirms the UV photon response.

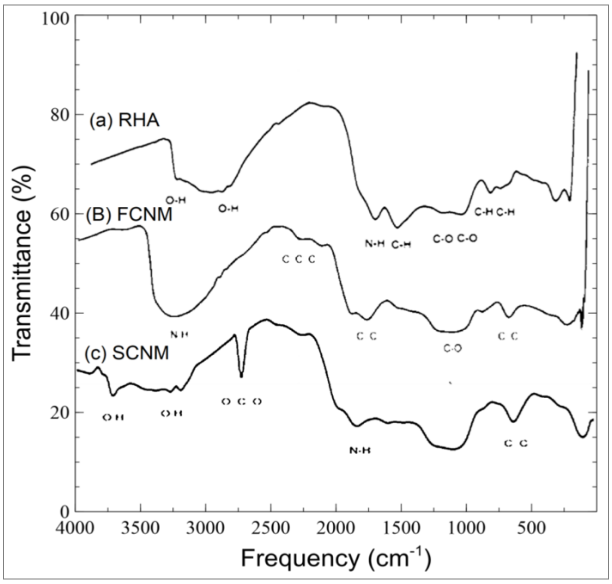

Figure 6. The FTIR characterization of: (a) RHA; (b) SCNM; (c) FCNM

The –OH and C=O functional groups in both FCNM and SCNM, indicating surface oxidation following bio-activation with bromelain. These polar groups play a critical role in modulating electron interactions at the semiconductor interface. In the context of CuO and SiO_2 surfaces, the –OH and C=O moieties are known to function as shallow electron traps or weak donors, facilitating temporary charge separation and suppressing rapid recombination. This interaction enhances charge mobility, thereby contributing to the elevated photocurrent generation observed in FCNM and SCNM. Given that excessive surface functionalization can also lead to recombination centers, the enhanced photocurrent response in these samples suggests that the density and distribution of the –OH and C=O groups remained within an optimal range, acting predominantly as beneficial trap states or carrier donors.

The voltage produced from the photo current test shown in **Figure 7**. Both SCNM and FCNM are superior in voltage generation compared to RHA. FCNM generates more potential due to its reactivity around 365 nm UV wavelength as shown by the UV-Vis characterization results (**Figure 5**). The 365 nm UV light has a close synchronicity with the FCNM molecular orbital frequency.

The electromagnetic wave synchronicity with a resonance electron determines its capability to energize the electron. An energized electron is called excited which capable to leave its original orbital [42]. However, the generated potentials confirm the photonic property of the synthesized semiconducting material. The incidence photon interacts with the electrons on CuO and Si orbital which adds up the kinetic energy of the electrons. At a certain level, when the required energy is enough to jump from a valence band to conduction band the photocurrent can be generated.

The photoelectric effect test shows the voltage generated from the photo current test shown in **Figure 7**. Both SCNM and FCNM are superior in voltage generation compared to RHA. FCNM generates more potential due to its reactivity around 365 nm UV wavelengths as shown by the UV-Vis characterization results (**Figure 5**). The 365 nm UV light has a close synchronicity with the FCNM molecular orbital frequency.

The flow of the photocurrent is controlled by the electron-hole pair dynamics. More electron-hole pairs responsible for more light sensitive material which shown by the FCNM. FCNM is more light -sensitive compared to SCNM and RHA due to its higher photocurrent generation. High quantities of electron-hole pairs ensure the continuous current flow which makes FCNM more appealing for applicative utilization. This study paves the way for potential applications in sensors, energy devices, and other semiconductor-related technologies, harnessing the unique properties of bio-derived nanomaterials for practical implementation in cutting-edge technologies.

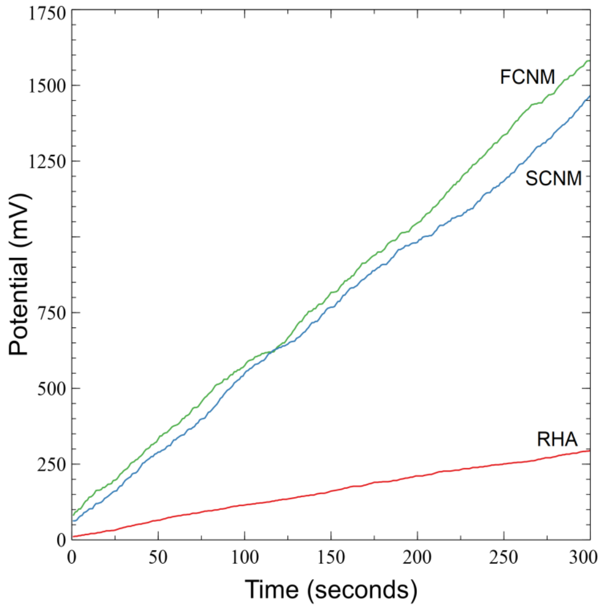

Figure 7. Voltage generated from photo current test

The interactions between carbon, CuO, and functional groups (e.g., –OH, C=O) with Si in SCNM and FCNM involve a combination of covalent (e.g., Si–O–Cu bridges), polar (dipole-dipole interactions via –OH/C=O with Cu^{2+}/Si^{4+}), and weak van der Waals forces. Covalent and polar bonds enhance charge delocalization and exciton lifetime by providing stable charge-transfer pathways, as evidenced by FTIR peaks (Si–O, C=O) and UV-Vis absorption (CuO bandgap). Weak van der Waals interactions, while structurally flexible, may introduce minor recombination centers. These bonding mechanisms collectively improve photoelectric stability, as observed in FCNM's sustained photocurrent response.

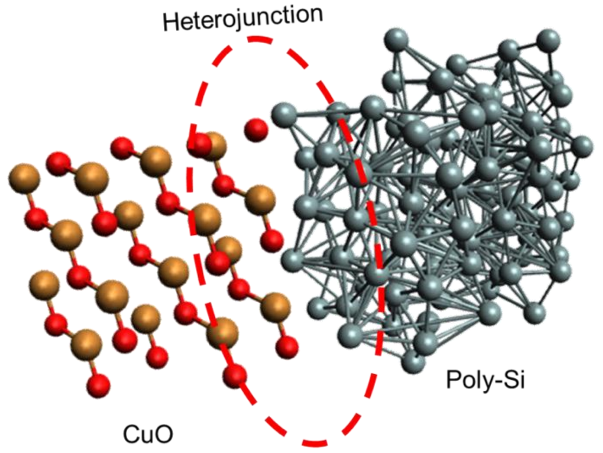

Figure 8. The illustration of heterojunction formation between P-Type CuO and N-type poly-silicon in the synthesized CNM

The observed photoelectric behavior of SCNM and FCNM can be fundamentally explained by the potential formation of heterojunctions between CuO and Si within their microstructures. A heterojunction occurs when two semiconductors with different band structures such as p-type CuO and n-type Si come into contact (see **Figure 8**) which creates an internal electric field at the interface [43]. This built-in field facilitates the separation of photogenerated electron–hole pairs, reducing recombination and thereby enhancing photocurrent generation. In the case of SCNM, the higher content of both Cu and Si detected by EDS, along with the strong UV absorption and high photocurrent response, suggests the formation of such localized p–n junctions. These junctions act as active sites for charge carrier movement under UV illumination, which explains the superior photoactivity of SCNM compared to RHA and FCNM. The improved charge separation efficiency contributes directly to the higher voltage output observed in the photoelectric test results.

The activation process using bromelain-rich pineapple extract introduced aromatic amino acid residues such onto the carbon surface. These residues, containing delocalized π-electron systems, may contribute to the formation of extended π–π conjugation across the carbon matrix [44]. This interaction facilitates partial electron delocalization, enhancing the electronic conductivity of the FCNM and SCNM materials. The observed increase in photocurrent and light absorption, particularly in the UV region, supports the hypothesis that π-conjugated domains were formed and contributed to improved charge mobility. These aromatic groups may act as bridges between semiconducting domains, allowing resonance-assisted charge transfer, which synergistically improves the overall electronic response of the composite. This mechanism aligns with previously reported behavior of carbon-based materials doped with aromatic structures, further supporting the enhanced photoactivity observed in FCNM and SCNM.

The comparison highlights that our FCNM (rice husk carbon/CuO-Si bio-activated by pineapple juice) offers a unique balance of eco-friendly synthesis and intrinsic photoelectric activity, unlike polyimide/silica composites (no photoresponse) or energy-intensive SiC derivatives (**Table 1**). While TiO_2/RHCNS composites exhibit superior visible-light performance, they rely on complex sol-gel processing and external TiO_2, whereas FCNM's bio-activated CuO/Si heterojunctions enable simpler, waste-derived semiconductor functionality. FCNM's UV-specific response (bandgap ~4.0–4.1 eV) and low-cost synthesis position it as a sustainable alternative for UV-sensitive applications, though future work could address its spectral limitations through doping or heterostructure engineering to compete with visible-light systems like TiO_2/RHCNS.

The presence of semiconducting oxide forms, specifically CuO and SiO_2, is supported by several characterizations. While EDS offers only surface-sensitive elemental data, it indicated the co-existence of Cu and Si across all samples (**Figure 3**). However, to confirm their chemical states, complementary spectroscopic techniques were employed. UV-Vis spectroscopy results showed strong absorption peaks in the UV region near 365 nm (**Figure 5**), particularly in SCNM and FCNM samples. This wavelength corresponds to the characteristic bandgap transition of CuO, supporting the presence of photoactive CuO phases. Furthermore, FTIR spectra (**Figure 6**) revealed bands associated with –OH and C=O functional groups, which are typical of oxidized carbon surfaces. Although the FTIR spectral range does not fully capture Si–O vibrations, the absence of metallic Si signals and the known oxidative conditions during activation (bromelain in pineapple juice under acidic pH) suggest the likely formation of SiO_2. The photocurrent test (**Figure 7**) under 365 nm UV illumination provided functional confirmation, as both SCNM and FCNM exhibited strong photoelectric responses behavior that aligns with semiconducting oxide materials. FCNM, which had a higher Cu/Si ratio, also showed the highest photocurrent output, indicating its enhanced photoreactivity. These findings collectively support the conclusion that Cu and Si in the samples predominantly exist in their semiconducting oxide forms.

Table 1. Comparison of SCNM and FCNM performance with other organic semiconductors

Material	Synthesis Method	Key Properties	Advantages/Limitations	Ref
Rice husk carbon + CuO/Si (bio-activated by pineapple juice)	Bio-activation + separation	UV-active (365 nm), bandgap ~4.0–4.1 eV	**Advantages:** Eco-friendly, low-cost, tunable bandgap. **Limitations:** Requires UV activation.	This work
Rice husk silica + polyimide	Sol-gel + film casting	Bandgap ≥3.1 eV, hydrophilic, improved optical conductivity	**Advantages:** Flexible films, scalable. **Limitations:** No intrinsic photoresponse, requires polymer matrix.	[45]
Rice husk-derived SiC (whiskers, particles)	Carbothermal reduction (1200–1800 °C)	Wide-bandgap semiconductor (SiC: ~2.3–3.3 eV)	**Advantages:** High thermal/mechanical stability. **Limitations:** Energy-intensive synthesis.	[46]
Rice husk silica + TiO_2	Sol-gel + composite formation	Visible-light active, reduced carrier recombination	**Advantages:** Visible-light response. **Limitations:** Complex synthesis, requires TiO_2.	[47]

4. Conclusion

The comparative analysis of RHA, SCNM, and FCNM reveals distinct structural and electronic properties shaped by the activation process using bromelain from pineapple juice. SEM and elemental analysis confirm the clustered morphology and higher CuO-Si content in SCNM, which correlates with stronger band bending at defect sites indicative of deeper electronic trap states. In contrast, FCNM exhibits more distributed CuO/Si structures, leading to shallow traps and higher photocurrent generation. FTIR spectra further validate enhanced polar interactions in SCNM and FCNM, supporting the role of bromelain in capturing polar impurities. UV-Vis and photoelectric measurements confirm the presence and photoactivity of CuO, with FCNM showing superior optoelectronic performance. These findings demonstrate the potential of bio-activated CuO/Si nanomaterials, especially FCNM, as promising candidates for next-generation organic photodiodes, solar cell coatings, phototransistors, and photocatalysts, contributing valuable insight into low-cost, bio-assisted semiconductor development.

Acknowledgments

We would like to express our gratitude to Advance material laboratory Udayana University for their UV-Vis and FTIR characterization support. We also give special thanks to Faculty of Engineering Udayana University, Department of Mechanical Engineering Brawijaya University, and Faculty of Engineering Sanata Dharma University.

Authors' Declaration

Authors' contributions and responsibilities - Conceived and designed the experiment (N.M.D, I.G.N.N.S); Performed the experiments (N.M.D, W.S.N); Analyzed and interpreted the data (N.M.D, W.S.N, I.N.G.W, I.G.K.P, N.P.G.S, W.N.S), Wrote the original paper (N.M.D, W.S.N); Validation (S.P.G.G.T); supervision (N.P.G.S;I.N.G.W;W.N.S).

Funding – This study does not receive any funding.

Availability of data and materials - All data is available from the authors.

Competing interests - The authors declare no competing interests.

Additional information – No additional information from the authors.

References

[1] C. Liang *et al.*, "Novel semiconductor materials for advanced supercapacitors," *Journal of Materials Chemistry C*, vol. 11, no. 13, pp. 4288–4317, 2023, doi: 10.1039/d2tc04816g.

[2] X. Li *et al.*, "Simplified synthetic routes for low cost and high photovoltaic performance n-type organic semiconductor acceptors," *Nature Communications*, vol. 10, no. 1, 2019, doi: 10.1038/s41467-019-08508-3.

[3] R. Soenoko, Purnami, and F. G. Utami Dewi, "Second stage cross flow turbine performance," *ARPN Journal of Engineering and Applied Sciences*, vol. 12, no. 6, 2017.

[4] W. Wijayanti, M. N. Sasongko, and Purnami, "The calorific values of solid and liquid yields consequenced by temperatures of mahogany pyrolysis," *ARPN Journal of Engineering and Applied Sciences*, vol. 11, no. 2, pp. 917–921, 2016.

[5] X. Hu, G. Li, and J. C. Yu, "Design, fabrication, and modification of nanostructured semiconductor materials for environmental and energy applications," *Langmuir*, vol. 26, no. 5, pp. 3031–3039, 2010, doi: 10.1021/la902142b.

[6] B. Q. G. Le and T. L. H. Doan, "Trend in biodegradable porous nanomaterials for anticancer drug delivery," *WIREs Nanomedicine and Nanobiotechnology*, vol. 15, no. 4, p. e1874, Jul. 2023, doi: 10.1002/wnan.1874.

[7] N. Baig, "Two-dimensional nanomaterials: A critical review of recent progress, properties, applications, and future directions," *Composites Part A: Applied Science and Manufacturing*, vol. 165, p. 107362, Feb. 2023, doi: 10.1016/j.compositesa.2022.107362.

[8] Y. Wei, L. Zou, H. Wang, Y. Wang, and Q. Xu, "Micro/Nano-Scaled Metal-Organic Frameworks

and Their Derivatives for Energy Applications," *Advanced Energy Materials*, vol. 12, no. 4, p. 2003970, Jan. 2022, doi: 10.1002/aenm.202003970.

[9] J. Sans, L. Soler, M. Domínguez, and J. Llorca, "Transforming a Compact Disk into a Simple and Cheap Photocatalytic Nanoreactor," *ACS Omega*, vol. 3, no. 6, pp. 6971–6975, Jun. 2018, doi: 10.1021/acsomega.8b00739.

[10] P. Purnami, N. Willy Satrio, S. Supriyono, and I. N. G. Wardana, "Digitally controlled organic electrocatalyst for water electrolysis," *International Journal of Hydrogen Energy*, vol. 47, no. 23, pp. 11877–11893, Mar. 2022, doi: 10.1016/j.ijhydene.2022.01.203.

[11] A. H. Holtslag, E. F. Mc Cord, and G. H. Werumeusbuning, "Recording mechanism of overcoated metallized dye layers on polycarbonate substrates," *Japanese Journal of Applied Physics*, vol. 31, no. 2S, pp. 484–493, 1992, doi: 10.1143/JJAP.31.484.

[12] S. Mas'ud, A. M. Sulaiman, H. Syahputra, and P. Purnami, "the Effect of Addition Bisphenol-a-Polycarbonate From Cd-R Waste As a Catalyst for Hydrogen Production," *International Journal of Mechanical Engineering Technologies and Applications*, vol. 4, no. 2, pp. 104–116, 2023, doi: 10.21776/mechta.2023.004.02.1.

[13] A. M. Sulaiman, S. Mas'ud, A. N. Daroini, and P. Purnami, "the Effect of Electrode Coating From Bisphenol-a-Polycarbonate Cd-R Waste for Hydrogen Production," *International Journal of Mechanical Engineering Technologies and Applications*, vol. 4, no. 1, pp. 10–21, Jan. 2023, doi: 10.21776/mechta.2023.004.01.2.

[14] P. Purnami, W. winarto, Y. K. Sofi'i, W. S. Nugroho, and I. N. G. Wardana, "The enhancement of magnetic field assisted water electrolysis hydrogen production from the compact disc recordable waste polycarbonate layer," *International Journal of Hydrogen Energy*, 2023, doi: 10.1016/j.ijhydene.2023.01.329.

[15] W. S. Nugroho, R. R. Esiliy, P. Purnami, and Y. K. Sofi'i, "The impact of chaotic flux reflection field on hydrogen evolution reaction of water electrolysis," *International Journal of Mechanical Engineering Technologies and Applications*, vol. 5, no. 1, pp. 12–22, Jan. 2024, doi: 10.21776/mechta.2024.005.01.2.

[16] Z. Chen *et al.*, "A Transparent Electrode Based on Solution-Processed ZnO for Organic Optoelectronic Devices," *Nature Communications*, vol. 13, no. 1, 2022, doi: 10.1038/s41467-022-32010-y.

[17] U. Shankar, C. R. Gupta, D. Oberoi, B. P. Singh, A. Kumar, and A. Bandyopadhyay, "A facile way to synthesize an intrinsically ultraviolet-C resistant tough semiconducting polymeric glass for organic optoelectronic device application," *Carbon*, vol. 168, pp. 485–498, 2020, doi: 10.1016/j.carbon.2020.07.015.

[18] H. B. Lee, W.-Y. Jin, M. M. Ovhal, N. Kumar, and J.-W. Kang, "Flexible transparent conducting electrodes based on metal meshes for organic optoelectronic device applications: a review," *Journal of Materials Chemistry C*, vol. 7, no. 5, pp. 1087–1110, 2019, doi: 10.1039/c8tc04423f.

[19] H. Bronstein, C. B. Nielsen, B. C. Schroeder, and I. McCulloch, "The role of chemical design in the performance of organic semiconductors," *Nature Reviews Chemistry*, vol. 4, no. 2, pp. 66–77, Jan. 2020, doi: 10.1038/s41570-019-0152-9.

[20] S. Giannini and J. Blumberger, "Charge Transport in Organic Semiconductors: The Perspective from Nonadiabatic Molecular Dynamics," *Accounts of Chemical Research*, vol. 55, no. 6, pp. 819–830, Mar. 2022, doi: 10.1021/acs.accounts.1c00675.

[21] L. Hu, X. Liu, S. Dalgleish, M. M. Matsushita, H. Yoshikawa, and K. Awaga, "Organic optoelectronic interfaces with anomalous transient photocurrent," *Journal of Materials Chemistry C*, vol. 3, no. 20, pp. 5122–5135, 2015, doi: 10.1039/c5tc00414d.

[22] N. M. Dwidiani, N. P. G. Suardana, I. N. G. Wardana, W. N. Septiadi, and A. A. A. Suryawan, "The Prediction of Photoactive Semiconductor Potential of Bio-Activated Rice Husk Ash Using Analytical Method," *Journal of the Chinese Society of Mechanical Engineers*, vol. 45, no. 4, pp. 375–383, 2024.

[23] S. Rukzon, P. Chindaprasirt, and R. Mahachai, "Effect of grinding on chemical and physical properties of rice husk ash," *International Journal of Minerals, Metallurgy and Materials*, vol. 16, no. 2, pp. 242–247, Apr. 2009, doi: 10.1016/S1674-4799(09)60041-8.

[24] D. L. Zhang, "Processing of advanced materials using high-energy mechanical milling," *Progress in Materials Science*, vol. 49, no. 3–4, pp. 537–560, Jan. 2004, doi: 10.1016/S0079-

6425(03)00034-3.

[25] L. C. de Lencastre Novaes, A. F. Jozala, A. M. Lopes, V. de Carvalho Santos-Ebinuma, P. G. Mazzola, and A. Pessoa Junior, “Stability, purification, and applications of bromelain: A review,” *Biotechnology Progress*, vol. 32, no. 1, pp. 5–13, Jan. 2016, doi: 10.1002/btpr.2190.

[26] L. R. Domingo, “Molecular electron density theory: A modern view of reactivity in organic chemistry,” *Molecules*, vol. 21, no. 10, 2016, doi: 10.3390/molecules21101319.

[27] A. Borrelli, “The story of the Higgs boson: the origin of mass in early particle physics,” *European Physical Journal H*, vol. 40, no. 1, pp. 1–52, 2015, doi: 10.1140/epjh/e2014-50026-9.

[28] Z. F. Yao *et al.*, “Approaching Crystal Structure and High Electron Mobility in Conjugated Polymer Crystals,” *Advanced Materials*, vol. 33, no. 10, 2021, doi: 10.1002/adma.202006794.

[29] C. A. Doswell and P. M. Markowski, “Is buoyancy a relative quantity?,” *Monthly Weather Review*, vol. 132, no. 4, pp. 853–863, 2004, doi: 10.1175/1520-0493(2004)132<0853:IBARQ>2.0.CO;2.

[30] C. Vermillion, B. Glass, and A. Rein, “Lighter-than-air wind energy systems,” *Green Energy and Technology*, pp. 501–514, 2013, doi: 10.1007/978-3-642-39965-7_30.

[31] H. J. Kang, I. Kim, J. Choi, G. J. Lee, and B. J. Park, “A concept study for the buoyancy support system based on the fixed fire-fighting system for damaged ships,” *Ocean Engineering*, vol. 155, pp. 361–370, 2018, doi: 10.1016/j.oceaneng.2018.02.040.

[32] H. Z. Tan, L. A. Slivovsky, and A. Pentland, “A sensing chair using pressure distribution sensors,” *IEEE/ASME Transactions on Mechatronics*, vol. 6, no. 3, pp. 261–268, 2001, doi: 10.1109/3516.951364.

[33] Y. Ramdhun, M. Mohanta, T. Arunachalam, R. Gupta, and D. Verma, “Bromelain-loaded polyvinyl alcohol–activated charcoal-based film for wound dressing applications,” *Macromolecular Research*, vol. 31, no. 5, pp. 469–488, May 2023, doi: 10.1007/s13233-023-00119-8.

[34] M. Holyavka *et al.*, “Influence of UV radiation on molecular structure and catalytic activity of free and immobilized bromelain, ficin and papain,” *Journal of Photochemistry and Photobiology B: Biology*, vol. 201, p. 111681, Dec. 2019, doi: 10.1016/j.jphotobiol.2019.111681.

[35] Y. Fisal, N. Hamidi, and M. N. Sasongko, “Pyrolysis of corn cob biomass toward gaseous products on small capacity reactor,” *International Journal of Mechanical Engineering Technologies and Applications*, vol. 5, no. 1, pp. 87–95, 2024, doi: 10.21776/mechta.2024.005.01.9.

[36] M. Farid *et al.*, “Phytoremediation of contaminated industrial wastewater by duckweed (Lemna minor L.): Growth and physiological response under acetic acid application,” *Chemosphere*, vol. 304, p. 135262, Oct. 2022, doi: 10.1016/j.chemosphere.2022.135262.

[37] B. Sürücü, H. H. Güllü, M. Terlemezoglu, D. E. Yildiz, and M. Parlak, “Determination of current transport characteristics in Au-Cu/CuO/n-Si Schottky diodes,” *Physica B: Condensed Matter*, vol. 570, pp. 246–253, Oct. 2019, doi: 10.1016/j.physb.2019.06.024.

[38] A. A. Sirusi, J. H. Ross, X. Yan, and S. Paschen, “NMR study of Ba8Cu5SixGe41-x clathrate semiconductors,” *Physical Chemistry Chemical Physics*, vol. 17, no. 26, pp. 16991–16996, Jun. 2015, doi: 10.1039/c5cp02575c.

[39] V. Quaresima and M. Ferrari, “A Mini-Review on Functional Near-Infrared Spectroscopy (fNIRS): Where Do We Stand, and Where Should We Go?,” *Photonics*, vol. 6, no. 3, p. 87, Aug. 2019, doi: 10.3390/photonics6030087.

[40] M. Musyaroh, W. Wijayanti, M. N. Sasongko, and A. D. Rizaldy, “Efek Intermolecular Forces: Perubahan Physical Properties pada Campuran Premium dan Bio-Additive Orange Peel,” *Jurnal Rekayasa Mesin*, vol. 12, no. 1, p. 133, 2021, doi: 10.21776/ub.jrm.2021.012.01.15.

[41] Y. Keriti, R. Brahimi, Y. Gabes, S. Kaci, and M. Trari, “Physical and photo-electrochemical properties of CuO thin film grown on µc-Si:H/glass. Application to solar energy conversion,” *Solar Energy*, vol. 206, pp. 787–792, Aug. 2020, doi: 10.1016/j.solener.2020.05.072.

[42] J. G. Kim *et al.*, “Mapping the emergence of molecular vibrations mediating bond formation,” *Nature*, vol. 582, no. 7813, pp. 520–524, Jun. 2020, doi: 10.1038/s41586-020-2417-3.

[43] M. Lin, H. Chen, Z. Zhang, and X. Wang, “Engineering interface structures for heterojunction

photocatalysts," *Physical Chemistry Chemical Physics*, vol. 25, no. 6, pp. 4388–4407, 2023, doi: 10.1039/d2cp05281d.

[44] V. Anh Tran *et al.*, "Experimental and computational investigation on interaction mechanism of Rhodamine B adsorption and photodegradation by zeolite imidazole frameworks-8," *Applied Surface Science*, vol. 538, p. 148065, Feb. 2021, doi: 10.1016/j.apsusc.2020.148065.

[45] A. A. Ebnalwaled, A. H. Sadek, S. H. Ismail, and G. G. Mohamed, "Structural, optical, dielectric, and surface properties of polyimide hybrid nanocomposites films embedded mesoporous silica nanoparticles synthesized from rice husk ash for optoelectronic applications," *Optical and Quantum Electronics*, vol. 54, no. 11, 2022, doi: 10.1007/s11082-022-03976-2.

[46] Q. Cong, X. Zhu, Z. Ban, J. Li, Z. Cai, and L. Pei, "Silicon Carbide-based Materials from Rice Husk," *Current Nanoscience*, vol. 20, no. 4, pp. 585–595, Jul. 2024, doi: 10.2174/0115734137316974240620095136.

[47] P. Sarkar, S. A. Moyez, A. Dey, S. Roy, and S. K. K. Das, "Experimental investigation of photocatalytic and photovoltaic activity of titania/rice husk crystalline nano-silica hybrid composite," *Solar Energy Materials and Solar Cells*, vol. 172, pp. 93–98, 2017, doi: 10.1016/j.solmat.2017.07.021.